NASA TM-84500

NASA Technical Memorandum 84500

PRELIMINARY ANALYSIS OF STS-3 ENTRY HEAT-TRANSFER DATA FOR THE ORBITER WINDWARD CENTERLINE

David A. Throckmorton,
H. Harris Hamilton II,
and E. Vincent Zoby

June 1982

National Aeronautics and
Space Administration
Langley Research Center
Hampton, Virginia 23665

PRELIMINARY ANALYSIS OF STS-3 ENTRY HEAT-TRANSFER DATA FOR THE ORBITER WINDWARD CENTERLINE

David A. Throckmorton, H. Harris Hamilton II,
and E. Vincent Zoby

SUMMARY

A preliminary analysis of heat-transfer data on the Space Shuttle Orbiter windward centerline for the STS-3 mission entry is presented. The paper includes temperature-time history plots for each measurement location, and tabulated wall-temperature and convective heating-rate data at 21 selected trajectory points. The STS-3 flight data are also compared with the predictions of two appproximate methods for computing convective heat-transfer rates in equilibrium air. The paper is intended to provide the technical community with early access to a wide range of orbiter heat-transfer data.

INTRODUCTION

Temperature measurements obtained at the aerodynamic surface of the orbiter's thermal protection system (TPS) provide for determination of the aerothermodynamic environment to which the orbiter is subjected during entry from Earth orbit. The measured temperatures are used in a rigorous analysis of heat conduction within, and reradiation from, the TPS in order to determine convective heat-transfer rates. Convective heating-rate data for the orbiter's windward centerline from the STS-3 mission entry are presented. The flight data are compared with the results of two approximate methods for computing convective heat-transfer rates.

SYMBOLS AND ACRONYMS

DFI	development flight instrumentation
h	altitude
M_∞	free-stream Mach number
P_∞	free-stream pressure
q_C	convective heat-transfer rate
TPS	thermal protection system
T_W	TPS surface temperature
T_∞	free-stream temperature

x/L	non-dimensional body length (L=32.89 m)
U_∞	free-stream velocity
α	angle-of-attack
ρ_∞	free-stream density

DATA SOURCE

During the orbital flight test missions, the orbiter has onboard an instrumentation system referred to as the development flight instrumentation (DFI). The DFI is comprised of over 4500 sensors, associated data-handling electronics, and recorder, which provide data to enable postflight certification of orbiter subsystems design. Included among the DFI are measurements of the orbiter's aerodynamic surface temperature at over 200 surface locations. These measurements are obtained from thermocouples mounted within the thermal protection system, in thermal contact with the aerodynamic surface coating. Sixteen of these thermocouples are located along the vehicle's windward centerline (fig. 1). DFI thermal data are recorded once each second throughout the entry time period. The measured temperature-time histories provide for determination of surface heat-transfer rates.

CONVECTIVE HEATING-RATE DETERMINATION

The measured time-histories of surface temperature are smoothed and subjected to an interactive review process to assure that the smoothed data provide an accurate representation of the raw temperature data. An inverse, one-dimensional, transient analysis of heat conduction within the TPS, and reradiation from the TPS surface, is used to determine convective heat-transfer rates (ref. 1). The uncertainty of heating rates determined by this method has been assessed (ref. 1) to be less than $\pm$ 10 percent.

ANALYTICAL TECHNIQUES

The approximate heating method of Zoby (ref. 2) uses a rapid inviscid flow-field procedure, laminar and turbulent heating equations which can be computed for constant or variable-entropy edge conditions, and equilibrium-air correlations. The flow environment along the windward centerline of the orbiter is approximated by using an equivalent axisymmetric body. Resulting heating-rate calculations have been validated for both laminar and turbulent flow conditions by comparison with experimental ground-test data and results of more rigorous predictions (refs. 3 and 4) at shuttle flight design conditions. It has previously been used in the analysis of orbiter entry heating data (refs. 5 and 6).

The approximate heating method of Hamilton (ref. 7) is based on a "local infinite swept cylinder analysis" which can be used to calculate both laminar and turbulent heating rates on the windward side of the orbiter. The method includes both equilibrium-air thermodynamic properties and variable boundary-layer-edge entropy. It has been shown to be in good agreement with wind-tunnel data, and has also been previously used in the analysis of orbiter entry heating data (ref. 7).

STS-3 RESULTS

Temperature Data

Smoothed temperature-time histories are shown in figure 2. The measurement location at x/L = 0.285 is part of an experiment (ref. 8) to investigate heating within gaps between TPS tiles. Data are not presented for the measurements at x/L = 0.297 and 0.402 as these measurements were part of an experiment (ref. 9) to investigate the catalytic efficiency of the TPS surface coating material. Data are presented, however, for a measurement which is located at x/L = 0.401, but 1.14 meters off of the plane of symmetry. No data are presented for the measurements located at x/L = 0.691 and 0.946, as these instruments did not operate properly on STS-3.

Heat-Transfer Data

Windward centerline convective heat-transfer data, determined by the method of reference 1, are tabulated in Table I for 21 trajectory points. These trajectory points span the entire portion of the entry which is of aerothermodynamic interest. The first points are prior to peak aerodynamic heating, and the last point is after boundary-layer transition has occurred over 90 percent of the vehicle's windward centerline.

Flight Environment Definition - Table I also contains information which describes the flight environment at each trajectory point. Determination of the flight environment parameters was accomplished through a process of reconstruction of the orbiter entry trajectory, modeling of the atmosphere on the day of entry, and correlation of these two data sets to provide an analytically-consistent definition of the entry flight environment. The vehicle state parameters of altitude, velocity, and angle of attack were determined through the trajectory reconstruction process of reference 10. Free-stream temperature was determined by the process of reference 11, which combines atmospheric modeling with direct measurement of atmospheric profiles on the day of entry. Atmospheric density was determined through a correlation of local surface pressure coefficient with free-stream dynamic pressure. The correlation function was generated using both wind-tunnel and flow-field computational results. Aerodynamic surface pressure was measured at a point on the windward

centerline at x/L = 0.025. The measured pressure was input to the correlation function in order to determine dynamic pressure.* Consideration of the vehicle velocity then provided for the determination of the atmospheric density. Free-stream pressure was determined by applying the gas law to the temperature and density data. The flight environment information contained in Table I was used as input to the analytical methods in generating the flight predictions to be discussed in the following section.

Heat-Transfer Distributions

Flight-measured heat-transfer distributions at five trajectory points, along with the approximate equilibrium-chemistry predictions of Hamilton and Zoby, are shown in figure 3. At time = 270 seconds, (fig. 3(a)), the flight data on the forward portion of the vehicle are as much as 35-percent lower than the equilibrium predictions; while on the aft portion of the vehicle, the flight data and predictions are in relatively good agreement. The large disparity between prediction and flight data on the forward portion of the vehicle is attributed to nonequilibrium chemistry in the shock layer in flight.

At time = 350 seconds (fig. 3(b)), the comparison between predictions and flight data is similar to that for the previous time. However, note that the data point at x/L = 0.166 is substantially higher than the surrounding data. The TPS tile which contains this measurement was previously coated with a highly catalytic material on STS-2, as part of the experiment of reference 9. Although the coating was cleaned from this tile prior to STS-3, the STS-3 data indicate that the catalytic efficiency of the surface of this tile remains greater than that of the surrounding baseline instrumented tiles.

In figure 3(c), time = 640 seconds, heating to the forward portion of the vehicle has increased substantially from the levels observed at the previous time, and downstream of x/L = 0.10, approaches the levels of the equilibrium predictions. The increased heating is probably the result of increased catalytic efficiency of the tile surface due to surface contamination--the contamination resulting from the melting of an acoustic-sensor cover at this location and deposition of melted material on the surface of the thermally-instrumented tiles downstream. Acoustic sensors are located on the vehicle centerline at x/L = 0.106 and x/L = 0.204. Postflight visual inspection of the TPS confirms that these sensors are a source of TPS contamination. The apparent occurrence, in time, of the contamination is evidenced by a sudden and significant temperature rise which occurs at a time of 520 seconds (figs. 2(e) and (g)). This phenomenon was previously observed at several centerline measurement locations on STS-2 (ref. 6).

---

*The correlation of local pressure coefficient with free-stream dynamic pressure was performed by R. C. Blanchard of the Langley Research Center and is to be described in a future publication.

At the later times (figs. 3(d) and (e)), the agreement between flight data and equilibrium-chemistry predictions becomes progressively better. It should be noted, however, that on STS-2 at approximately the same altitude/velocity/angle-of-attack condition as that of figure 3(e), nonequilibrium predictions indicate that significant nonequilibrium effects should still be evident in the heat-transfer data (ref. 12). Also, on STS-2, the coated tiles of the Catalytic Surface Experiment (ref. 13) provided evidence of nonequilibrium chemistry effects in the boundary layer at similar flight conditions.

CONCLUDING REMARKS

A preliminary analysis of orbiter windward-centerline heat-transfer data from the STS-3 mission entry is presented. The flight data were compared with the predictions of two appproximate methods for computing convective heat-transfer rates in air in chemical equilibrium. The comparisons indicate that at altitudes greater than 60 kilometers, flight heat-transfer rates are significantly influenced by nonequilibrium chemistry effects. At altitudes below 60 kilometers, the flight data and equilibrium chemistry predictions are in good agreement. However, even at these conditions, other computations and experiment indicate that significant nonequilibrium chemistry effects should still be evident.

REFERENCES

1. Throckmorton, D. A.: Benchmark Aerodynamic Heat Transfer Data from the First Flight of the Space Shuttle Orbiter. AIAA Paper 82-0003, January 1982.

2. Zoby, E. V.; Moss, J. N.; and Sutton, K.: Approximate Convective Heating Equations for Hypersonic Flows. Journal of Spacecraft and Rockets, vol.18, no. 1, January 1981.

3. Rakich, J. V.; and Lanfranco, M. J.: Numerical Computation of Space Shuttle Laminar Heating and Surface Streamlines. Journal of Spacecraft and Rockets, vol. 14, no.5, May 1977.

4. Goodrich, W. D.; Li, C. P.; Houston, C. K.; Chiu, P. B.; and Olmedo, L.: Numerical Computations of Orbiter Flowfields and Laminar Heating Rates. Journal of Spacecraft and Rockets, vol. 14, no. 5, May 1977.

5. Zoby, E. V.: Comparisons of Free-flight Experimental and Predicted Heating Rates for the Space Shuttle. AIAA Paper 82-0002, January 1982.

6. Zoby, E. V.: Analysis of STS-2 Experimental Heating Rates and Transition Data. AIAA Paper 82-0822, June 1982.

7. Hamilton, H. H. II: Approximate Method of Predicting Heating on the Windward Side of Space Shuttle Orbiter and Comparisons to Flight Data. AIAA Paper 82-0823, June 1982.

8. Pitts, W. C.: Flight Measurements of Tile Gap Heating on the Space Shuttle. AIAA Paper 82-0840, June 1982.

9. Stewart, D. A.; and Rakich, J. V.: Catalytic Surface Effects Experiment on Space Shuttle. AIAA Paper 81-1143, June 1981.

10. Compton, H. R.; Findlay, J. T.; Kelly, G. M.; and Heck, M.L.: Shuttle (STS-1) Entry Trajectory Reconstruction. AIAA Paper 81-2459, November 1981.

11. Price, J. M.; and Blanchard, R. C.: Determination of Atmospheric Properties for STS-1 Aerothermodynamic Investigations. AIAA Paper 81-2430, November 1981.

12. Shinn, J. L.; Moss, J. N.; and Simmonds, A. L.: Viscous Shock Layer Heating Analysis for the Shuttle Windward Plane with Surface Finite Catalytic Recombination Rates. AIAA Paper 82-0842, June 1982.

13. Rakich, J. V.; and Stewart, D. A.: Results of a Flight Experiment on the Catalytic Efficiency of the Space Shuttle Heat Shield. AIAA Paper 82-0944, June 1982.

Table I - STS-3 Windward Centerline Heat Transfer

Time = 225	secs	M_∞ = 26.7	
h = 88.1	km	P_∞ = 0.28	N/m^2
u_∞ = 7.44	km/sec	T_∞ = 193	K
α = 40.1	degrees	ρ_∞ = 4.96 x 10^{-6}	kg/m^3

x/L	T_w (K)	q_c (kW/m^2)
0.025	1055	77.5
0.098	884	40.1
0.140	838	33.2
0.166	829	32.6
0.194	767	26.2
0.255	791	27.0
0.285	770	25.4
0.401	764	23.9
0.497	732	22.0
0.592	741	22.0
0.795	692	18.0
0.894	656	14.5
0.986	572	9.0

Table I - Continued.

Time = 245	secs	M_∞ = 26.9	
h = 85.3	km	P_∞ = 0.43	N/m^2
u_∞ = 7.47	km/sec	T_∞ = 192	K
α = 39.4	degrees	ρ_∞ = 7.78 x 10^{-6}	kg/m^3

x/L	T_w (K)	q_c (kW/m^2)
0.025	1136	98.2
0.098	963	51.5
0.140	909	42.0
0.166	901	39.6
0.194	858	34.9
0.255	868	35.9
0.285	864	36.2
0.401	831	29.4
0.497	822	30.5
0.592	815	28.7
0.795	763	23.7
0.894	726	19.8
0.986	642	14.0

Table I - Continued.

Time = 270	secs	M_∞ = 27.1	
h = 82.2	km	P_∞ = 0.70	N/m^2
u_∞ = 7.52	km/sec	T_∞ = 192	K
α = 39.5	degrees	ρ_∞ = 1.28 x 10^{-5}	kg/m^3

x/L	T_w (K)	q_c (kW/m^2)
0.025	1203	121.
0.098	1027	64.2
0.140	974	51.9
0.166	957	49.0
0.194	934	45.6
0.255	938	46.5
0.285	949	46.9
0.401	902	40.5
0.497	902	40.2
0.592	883	36.2
0.795	851	33.9
0.894	799	26.7
0.986	715	19.2

Table I - Continued.

Time = 300	secs	M_∞ = 26.9	
h = 79.0	km	P_∞ = 1.17	N/m^2
u_∞ = 7.50	km/sec	T_∞ = 194	K
α = 41.0	degrees	ρ_∞ = 2.09 x 10^{-5}	kg/m^3

x/L	T_w (K)	q_c (kW/m^2)
0.025	1266	144.
0.098	1082	76.8
0.140	1039	66.5
0.166	1037	67.0
0.194	1001	58.2
0.255	1008	59.5
0.285	979	52.7
0.401	972	52.1
0.497	962	49.8
0.592	938	45.5
0.795	941	47.4
0.894	890	39.4
0.986	686	10.7

Table I - Continued.

Time = 350	secs	M_∞ = 26.2	
h = 76.2	km	P_∞ = 1.90	N/m^2
u_∞ = 7.40	km/sec	T_∞ = 199	K
α = 39.6	degrees	ρ_∞ = 3.32 x 10^{-5}	kg/m^3

x/L	T_w (K)	q_c (kW/m^2)
0.025	1324	168.
0.098	1124	86.7
0.140	1108	81.7
0.166	1193	112.
0.194	1051	67.3
0.255	1048	66.2
0.285	1019	59.4
0.401	1016	58.6
0.497	1009	57.3
0.592	1002	56.5
0.795	1017	59.1
0.894	971	50.2
0.986	647	10.4

Table I - Continued.

Time = 415	secs	M_∞ = 25.5	
h = 74.7	km	P_∞ = 2.40	N/m^2
u_∞ = 7.26	km/sec	T_∞ = 202	K
α = 40.1	degrees	ρ_∞ = 4.14 x 10^{-5}	kg/m^3

x/L	T_w (K)	q_c (kW/m^2)
0.025	1345	176.
0.098	1147	93.3
0.140	1162	98.4
0.166	1233	123.
0.194	1077	73.2
0.255	1077	72.7
0.285	1048	65.7
0.401	1043	64.7
0.497	1034	62.4
0.592	1057	68.2
0.795	1051	67.0
0.894	996	54.0
0.986	703	14.6

Table I - Continued.

Time = 495	secs	M_∞ = 24.5	
h = 73.1	km	P_∞ = 3.22	N/m^2
u_∞ = 7.05	km/sec	T_∞ = 207	K
α = 39.6	degrees	ρ_∞ = 5.42 x 10^{-5}	kg/m^3

x/L	T_w (K)	q_c (kW/m^2)
0.025	1357	182.
0.098	1165	98.2
0.140	1194	109.
0.166	1217	116.
0.194	1105	80.1
0.255	1100	79.0
0.285	1082	73.9
0.401	1056	67.2
0.497	1052	66.5
0.592	1069	70.4
0.795	1069	71.0
0.894	1002	54.7
0.986	713	14.5

Table I - Continued.

Time = 640	secs	M_∞ = 22.3	
h = 70.1	km	P_∞ = 5.10	N/m^2
u_∞ = 6.57	km/sec	T_∞ = 217	K
α = 40.1	degrees	ρ_∞ = 8.19 x 10^{-5}	kg/m^3

x/L	T_w (K)	q_c (kW/m^2)
0.025	1378	192.
0.098	1189	106.
0.140	1214	115.
0.166	1209	113.
0.194	1159	95.6
0.255	1130	85.9
0.285	1114	81.9
0.401	1076	71.8
0.497	1058	66.5
0.592	1057	66.1
0.795	1065	68.3
0.894	1002	54.1
0.986	664	10.8

Table I - Continued.

Time = 745	secs	M_∞ = 19.9	
h = 67.0	km	P_∞ = 8.25	N/m^2
u_∞ = 6.09	km/sec	T_∞ = 233	K
α = 39.9	degrees	ρ_∞ = 1.23 x 10^{-4}	kg/m^3

x/L	T_w (K)	q_c (kW/m^2)
0.025	1403	205.
0.098	1211	114.
0.140	1200	109.
0.166	1192	106.
0.194	1136	87.7
0.255	1113	81.3
0.285	1096	76.2
0.401	1064	67.9
0.497	1038	61.7
0.592	1033	60.4
0.795	1041	62.2
0.894	988	51.1
0.986	673	11.4

Table I - Continued.

Time = 825	secs	M_∞ = 17.9	
h = 64.0	km	P_∞ = 13.5	N/m^2
u_∞ = 5.66	km/sec	T_∞ = 249	K
α = 39.3	degrees	ρ_∞ = 1.89 x 10^{-4}	kg/m^3

x/L	T_w (K)	q_c (kW/m^2)
0.025	1424	217.
0.098	1222	117.
0.140	1187	104.
0.166	1178	101.
0.194	1116	81.4
0.255	1097	75.9
0.285	1081	71.8
0.401	1048	63.9
0.497	1021	57.5
0.592	1009	54.7
0.795	1028	59.1
0.894	982	49.6
0.986	664	10.8

Table I - Continued.

Time = 920	secs	M_∞ = 15.4	
h = 60.8	km	P_∞ = 20.9	N/m^2
u_∞ = 4.98	km/sec	T_∞ = 262	K
α = 43.0	degrees	ρ_∞ = 2.77 x 10^{-4}	kg/m^3

x/L	T_w (K)	q_c (kW/m^2)
0.025	1384	192.
0.098	1183	103.
0.140	1147	90.5
0.166	1145	89.9
0.194	1082	72.0
0.255	1052	64.4
0.285	1048	63.7
0.401	1016	56.2
0.497	982	48.9
0.592	955	43.9
0.795	981	48.9
0.894	963	45.7
0.986	662	9.2

Table I - Continued.

Time = 960	secs	M_∞ = 14.0	
h = 57.8	km	P_∞ = 31.4	N/m^2
u_∞ = 4.61	km/sec	T_∞ = 269	K
α = 40.9	degrees	ρ_∞ = 4.06 x 10^{-4}	kg/m^3

x/L	T_w (K)	q_c (kW/m^2)
0.025	1357	177.
0.098	1160	94.8
0.140	1121	82.4
0.166	1118	81.6
0.194	1058	65.7
0.255	1023	56.2
0.285	1023	57.5
0.401	989	50.2
0.497	962	44.9
0.592	923	38.1
0.795	936	40.2
0.894	944	42.2
0.986	635	8.7

Table I - Continued.

Time = 1015	secs	M_∞ = 12.3	
h = 55.0	km	P_∞ = 45.3	N/m^2
u_∞ = 4.07	km/sec	T_∞ = 272	K
α = 39.6	degrees	ρ_∞ = 5.80 x 10^{-4}	kg/m^3

x/L	T_w (K)	q_c (kW/m^2)
0.025	1295	145.
0.098	1102	76.7
0.140	1066	67.0
0.166	1054	62.5
0.194	1007	53.5
0.255	967	42.8
0.285	967	45.5
0.401	938	40.3
0.497	918	37.1
0.592	877	30.8
0.795	874	29.5
0.894	889	31.8
0.986	594	5.8

Table I - Continued.

Time = 1080	secs	M_∞ = 10.4	
h = 51.8	km	P_∞ = 65.4	N/m^2
u_∞ = 3.44	km/sec	T_∞ = 273	K
α = 38.9	degrees	ρ_∞ = 8.36 x 10^{-4}	kg/m^3

x/L	T_w (K)	q_c (kW/m^2)
0.025	1204	107.
0.098	1021	54.8
0.140	978	45.4
0.166	965	42.9
0.194	930	37.2
0.255	895	32.0
0.285	901	32.8
0.401	875	29.4
0.497	865	29.1
0.592	807	20.2
0.795	798	19.1
0.894	799	19.3
0.986	574	5.3

Table I - Continued.

Time = 1100	secs	M_∞ = 9.82	
h = 50.3	km	P_∞ = 86.7	N/m^2
u_∞ = 3.25	km/sec	T_∞ = 272	K
α = 38.0	degrees	ρ_∞ = 1.11 x 10^{-3}	kg/m^3

x/L	T_w (K)	q_c (kW/m^2)
0.025	1178	97.1
0.098	998	49.3
0.140	951	39.8
0.166	937	37.4
0.194	910	33.9
0.255	877	30.3
0.285	884	30.3
0.401	856	26.1
0.497	845	26.2
0.592	788	18.3
0.795	781	17.1
0.894	771	16.7
0.986	588	6.7

Table I - Continued.

Time = 1120	secs	M_∞ = 9.3	
h = 48.8	km	P_∞ = 94.5	N/m^2
u_∞ = 3.05	km/sec	T_∞ = 270	K
α = 36.4	degrees	ρ_∞ = 1.19 x 10^{-3}	kg/m^3

x/L	T_w (K)	q_c (kW/m^2)
0.025	1155	89.8
0.098	975	45.2
0.140	923	35.4
0.166	907	32.6
0.194	890	32.1
0.255	859	26.8
0.285	864	27.6
0.401	839	25.4
0.497	830	23.5
0.592	766	17.1
0.795	811	34.1
0.894	818	34.7
0.986	777	46.2

Table I - Continued.

Time = 1145	secs	M_∞ = 8.6	
h = 47.3	km	P_∞ = 114	N/m^2
u_∞ = 2.82	km/sec	T_∞ = 268	K
α = 33.6	degrees	ρ_∞ = 1.48 x 10^{-3}	kg/m^3

x/L	T_w (K)	q_c (kW/m^2)
0.025	1113	75.7
0.098	940	38.2
0.140	880	28.7
0.166	865	26.5
0.194	860	26.8
0.255	827	21.8
0.285	831	23.0
0.401	807	20.2
0.497	802	18.4
0.592	742	14.8
0.795	1021	51.1
0.894	967	40.1
0.986	953	47.8

Table I - Continued.

Time = 1180	secs	M_∞ = 7.7	
h = 45.8	km	P_∞ = 136	N/m^2
u_∞ = 2.51	km/sec	T_∞ = 266	K
α = 33.3	degrees	ρ_∞ = 1.79 x 10^{-3}	kg/m^3

x/L	T_w (K)	q_c (kW/m^2)
0.025	1042	56.2
0.098	881	28.3
0.140	824	20.6
0.166	810	19.7
0.194	813	20.0
0.255	772	16.4
0.285	786	17.5
0.401	762	15.7
0.497	756	15.3
0.592	975	56.3
0.795	1007	53.5
0.894	944	41.2
0.986	911	36.5

Table I - Continued.

Time = 1220	secs	M_∞ = 6.8	
h = 42.8	km	P_∞ = 203	N/m^2
u_∞ = 2.21	km/sec	T_∞ = 259	K
α = 29.6	degrees	ρ_∞ = 2.72 x 10^{-3}	kg/m^3

x/L	T_w (K)	q_c (kW/m^2)
0.025	972	41.6
0.098	820	20.5
0.140	941	42.1
0.166	936	39.8
0.194	929	39.6
0.255	924	39.1
0.285	924	39.3
0.401	928	40.1
0.497	937	41.2
0.592	940	40.4
0.795	947	40.9
0.894	889	31.6
0.986	858	27.8

Table I - Continued.

Time = 1260	secs	M_∞ = 6.01	
h = 39.6	km	P_∞ = 306	N/m^2
u_∞ = 1.91	km/sec	T_∞ = 252	K
α = 26.1	degrees	ρ_∞ = 4.23 x 10^{-3}	kg/m^3

x/L	T_w (K)	q_c (kW/m^2)
0.025	910	30.9
0.098	770	16.6
0.140	899	32.3
0.166	888	30.6
0.194	884	30.5
0.255	878	29.4
0.285	878	29.5
0.401	880	30.0
0.497	886	31.0
0.592	882	30.2
0.795	886	30.5
0.894	833	23.6
0.986	803	20.8

Table I - Concluded.

Time = 1300	secs	M_∞ = 5.2	
h = 36.5	km	P_∞ = 468	N/m^2
u_∞ = 1.63	km/sec	T_∞ = 244	K
α = 22.7	degrees	ρ_∞ = 6.70 x 10^{-3}	kg/m^3

x/L	T_w (K)	q_c (kW/m^2)
0.025	844	21.1
0.098	845	26.8
0.140	835	22.4
0.166	823	20.8
0.194	820	21.1
0.255	811	20.0
0.285	811	19.8
0.401	816	21.0
0.497	817	20.8
0.592	811	20.2
0.795	817	21.0
0.894	772	16.2
0.986	748	14.9

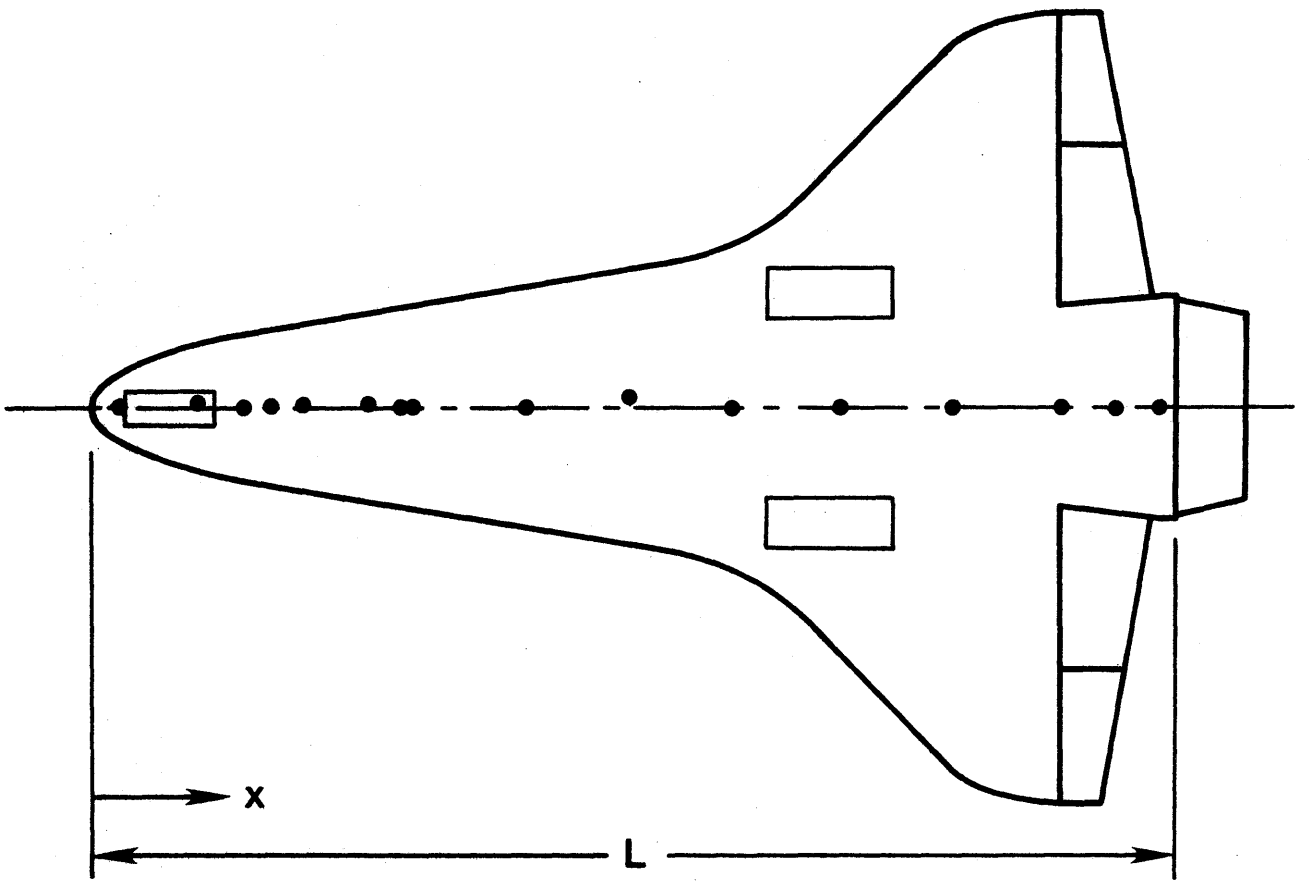

Figure 1. - Windward centerline surface temperature measurement locations.

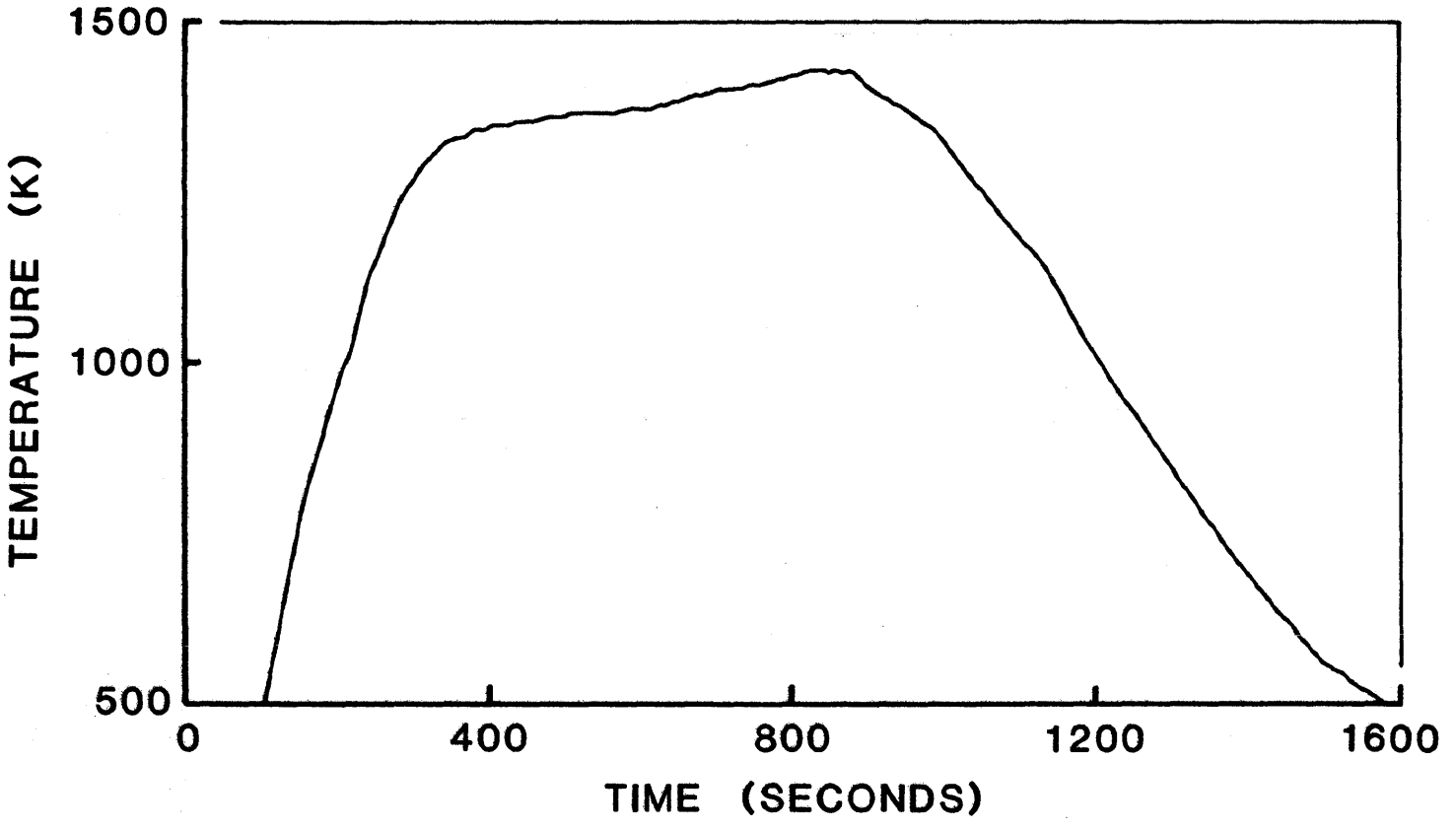

(a) x/L = 0.025

Figure 2. - STS-3 temperature-time histories.

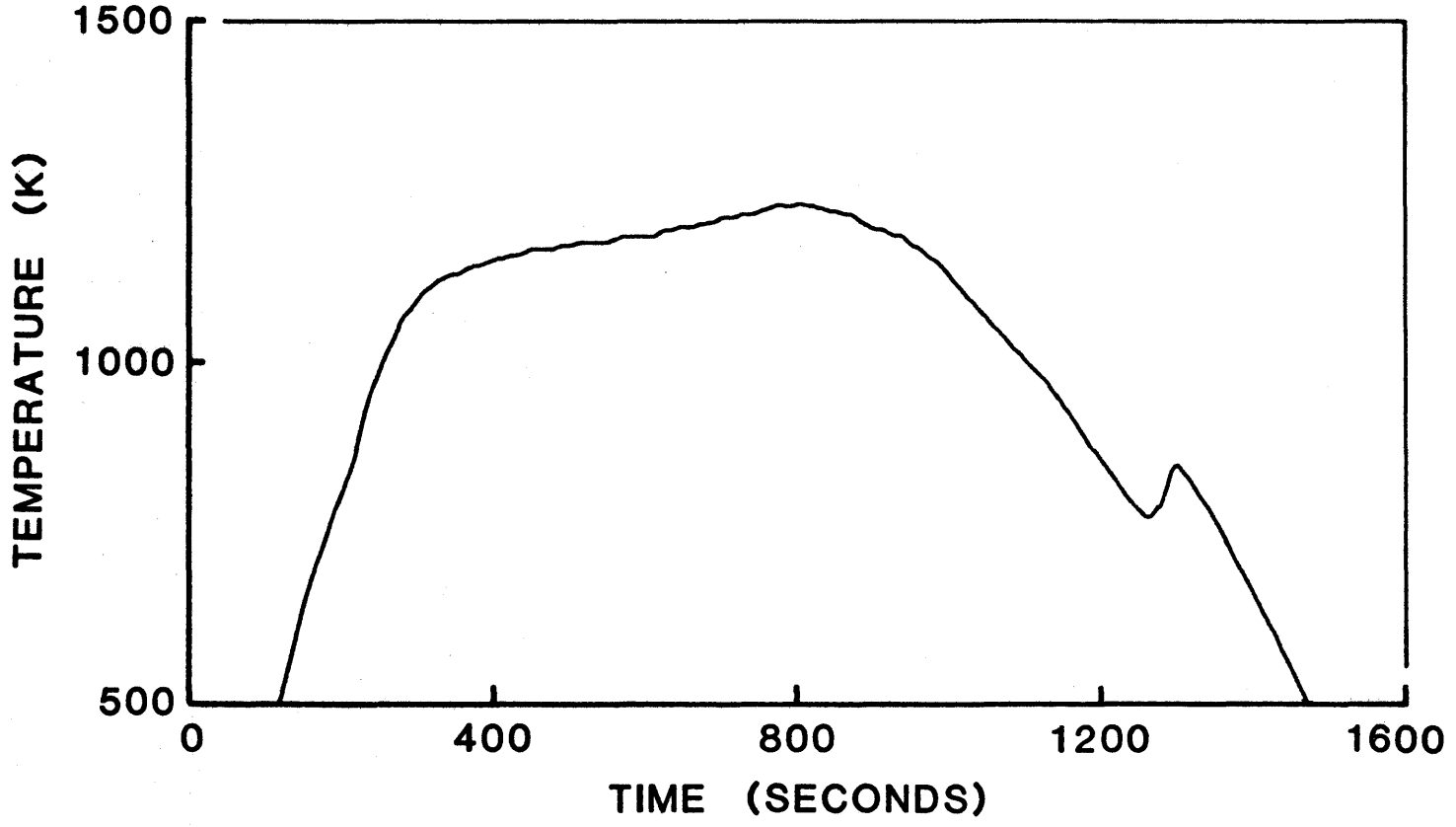

(b) x/L = 0.098

Figure 2. - Continued.

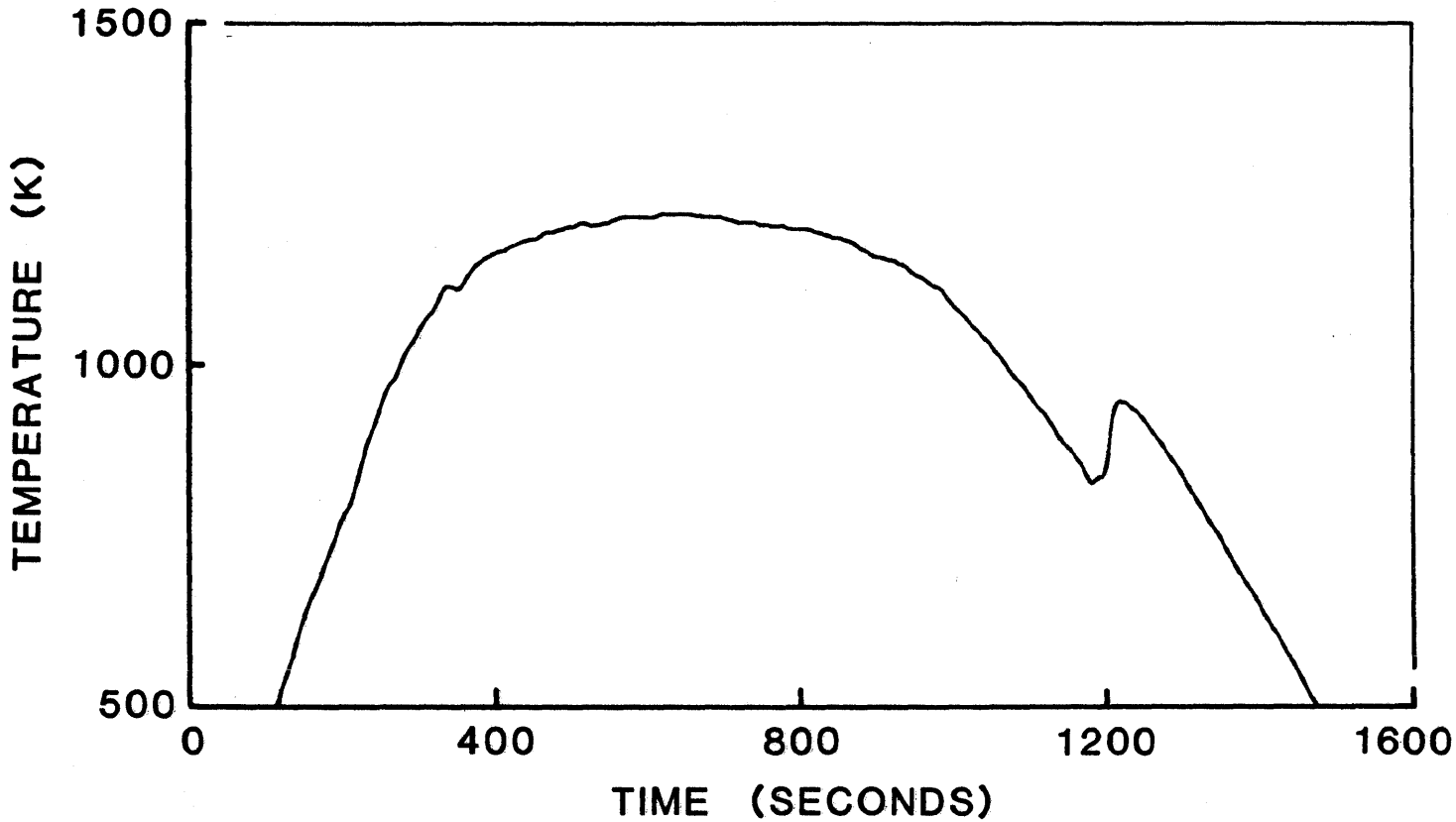

(c) x/L = 0.140

Figure 2. - Continued.

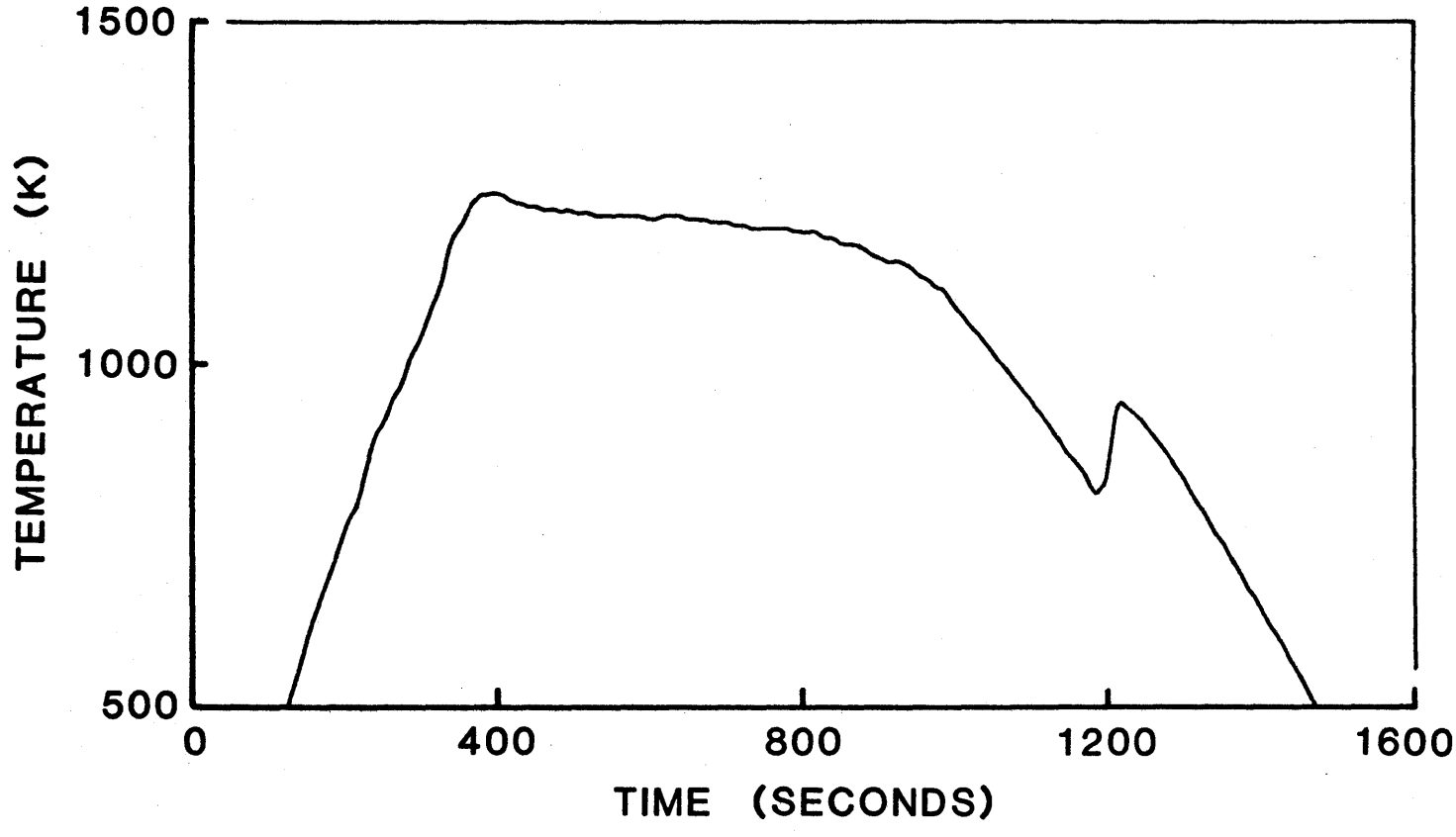

(d) x/L = 0.166

Figure 2. - Continued.

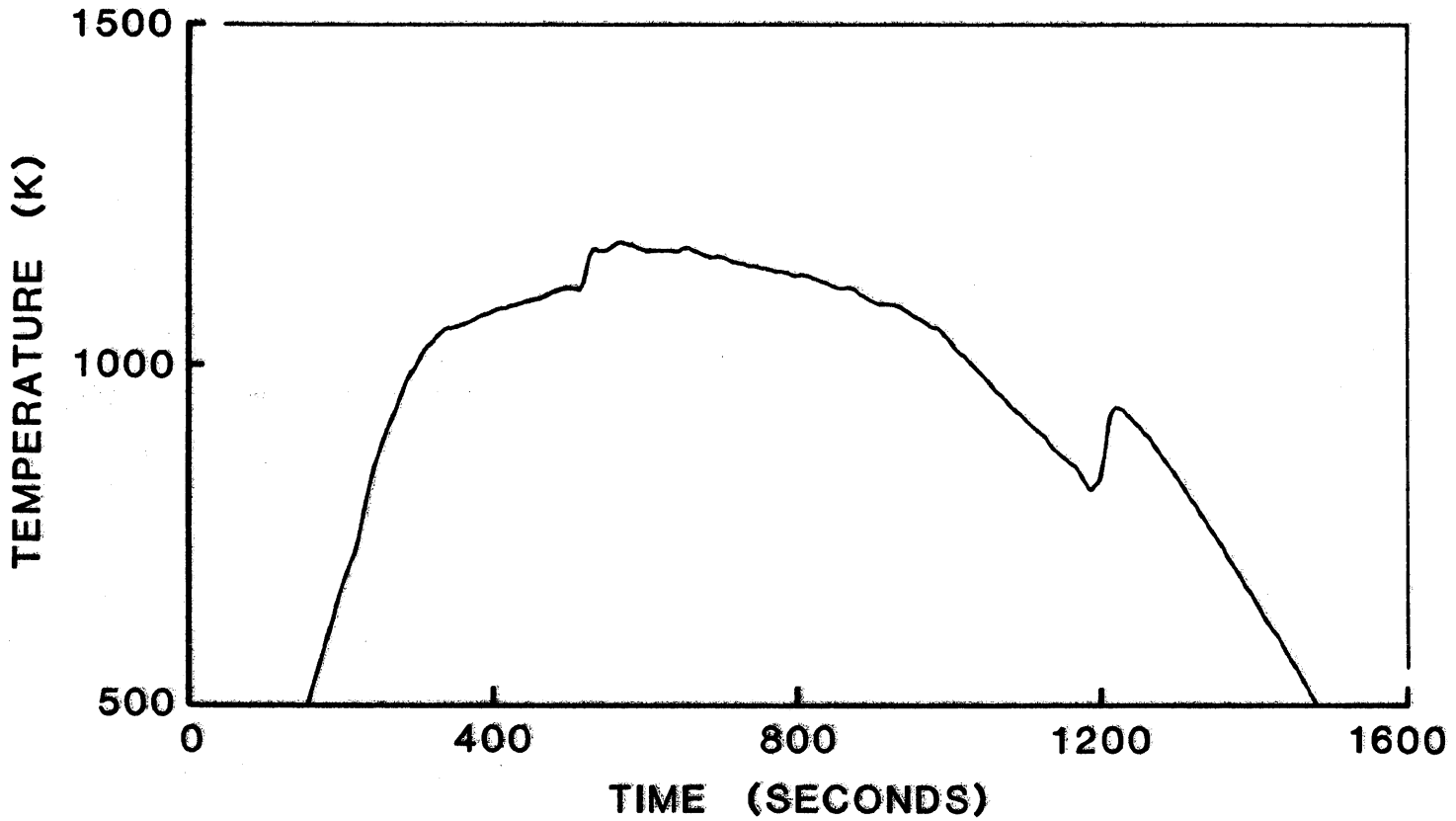

(e) x/L = 0.194

Figure 2. - Continued.

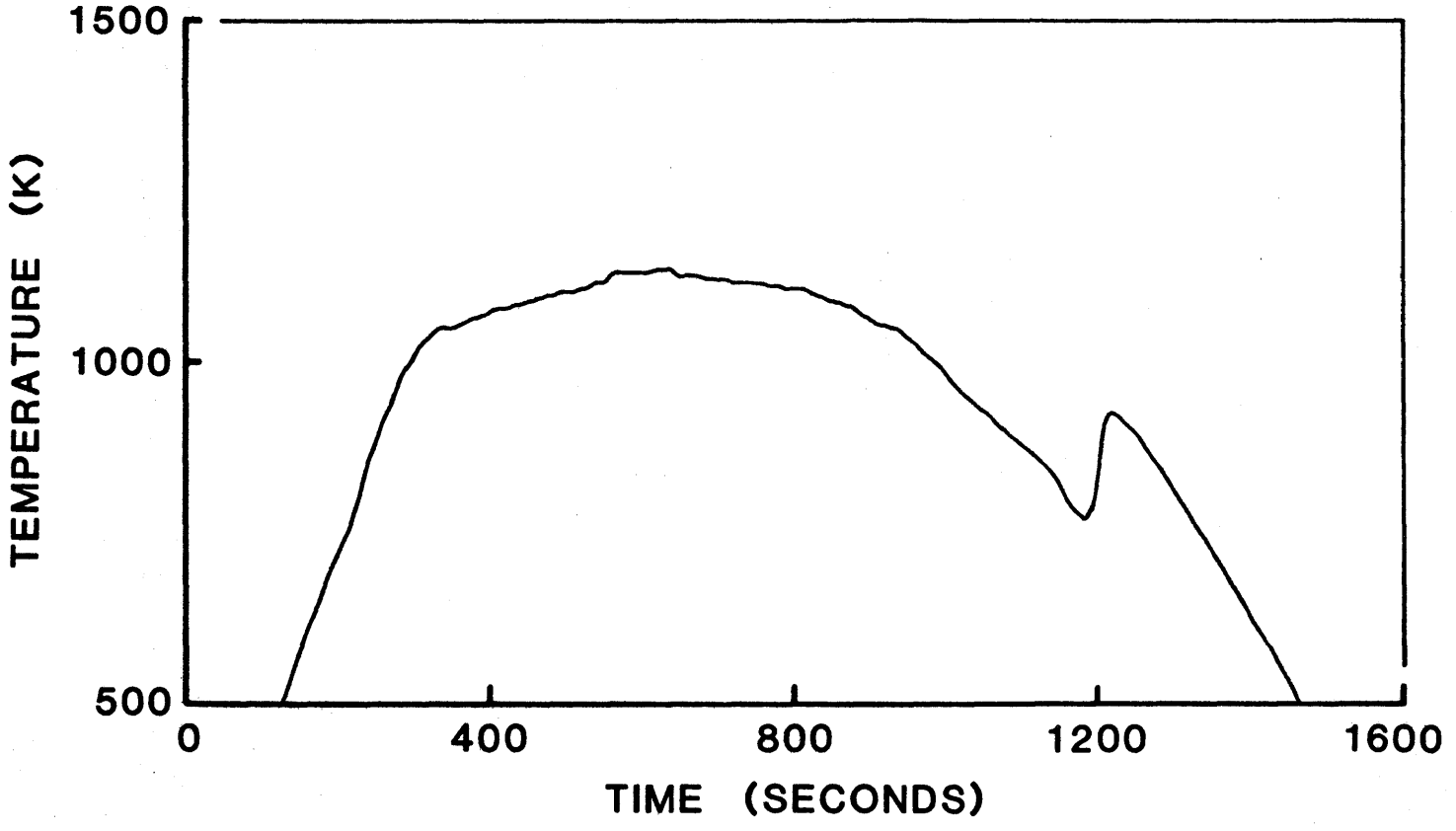

(f) x/L = 0.255

Figure 2. - Continued.

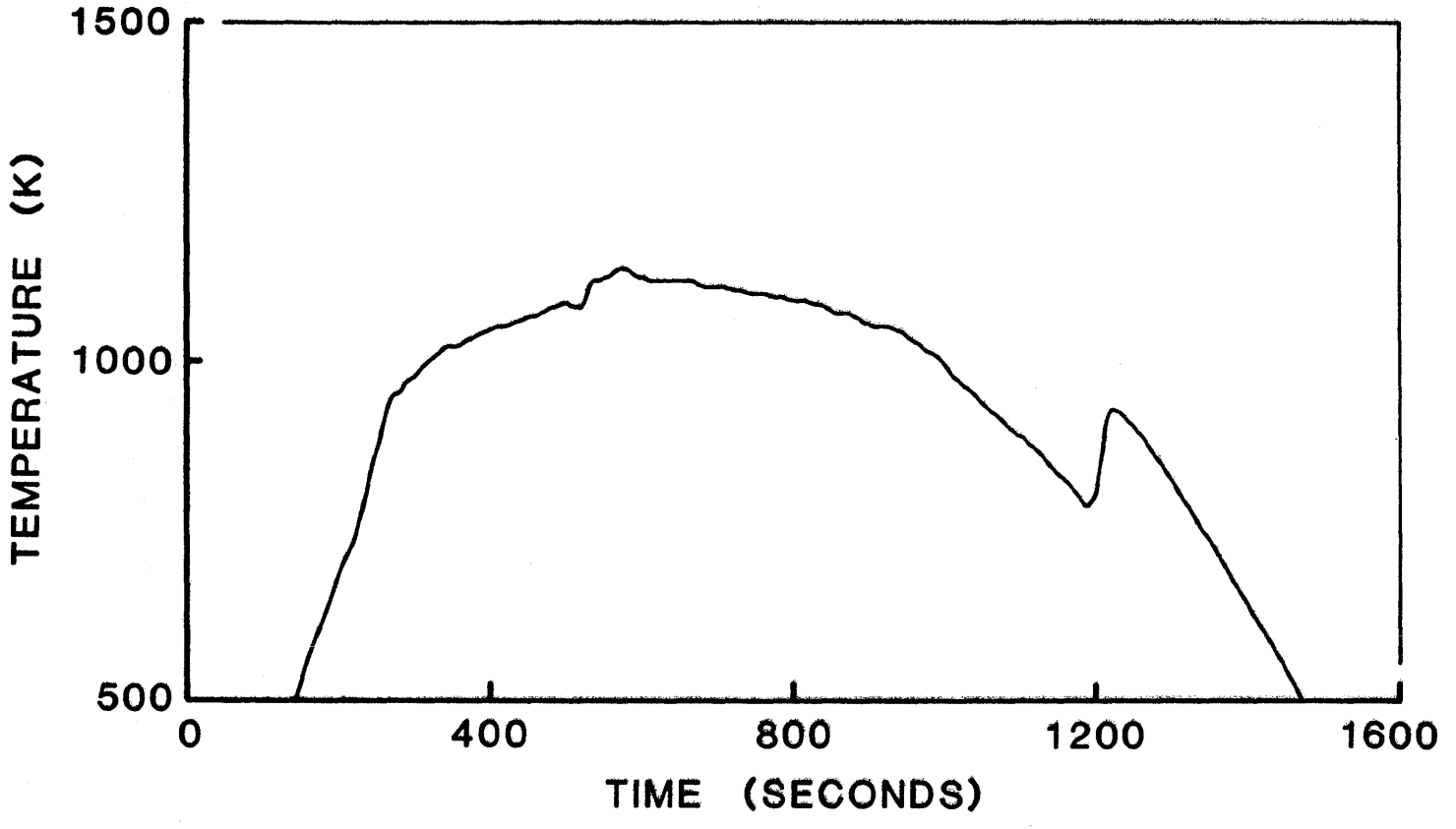

(g) x/L =0.285

Figure 2. - Continued.

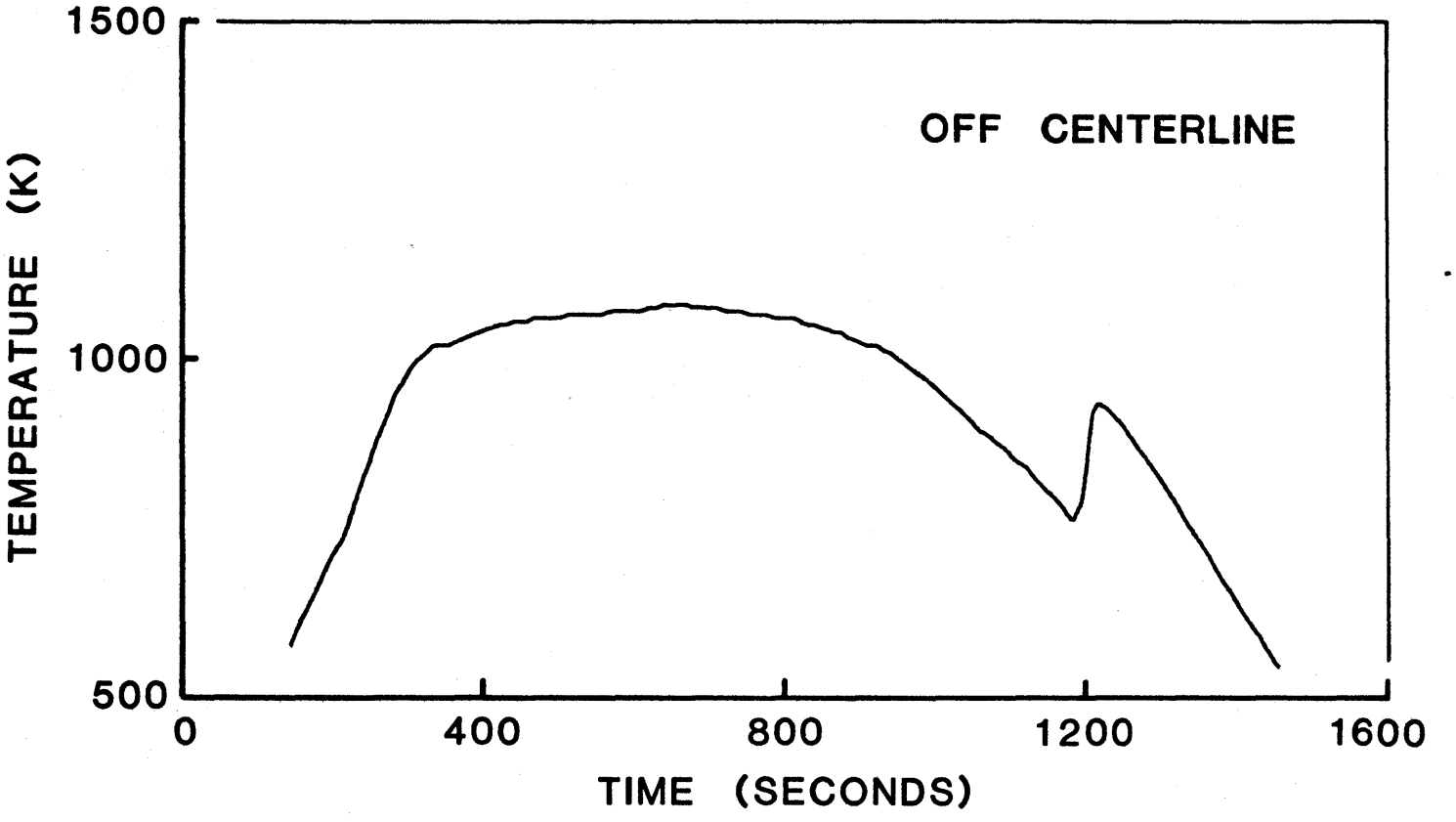

(h) x/L = 0.401

Figure 2. - Continued.

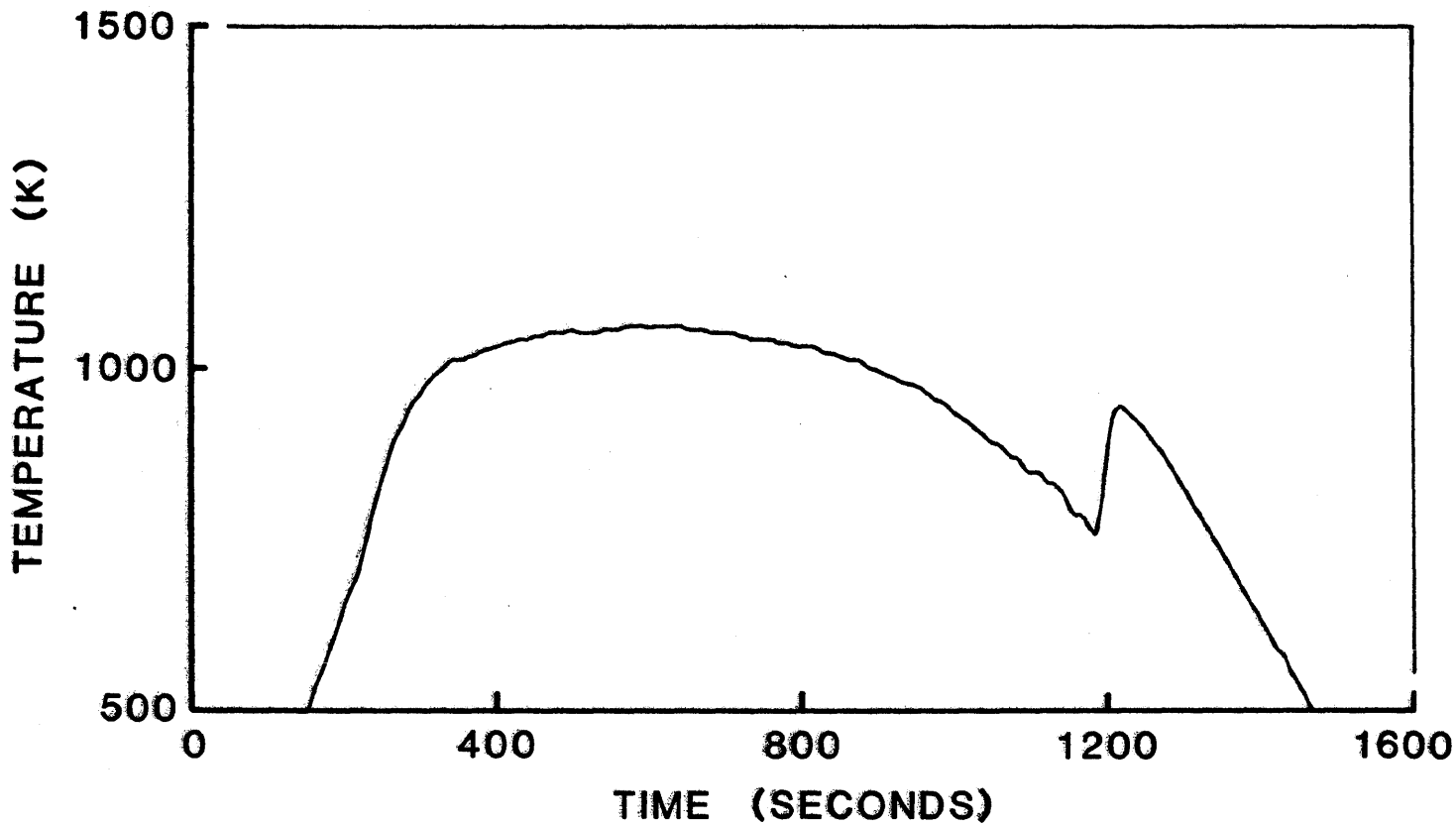

(i) x/L = 0.497

Figure 2. - Continued.

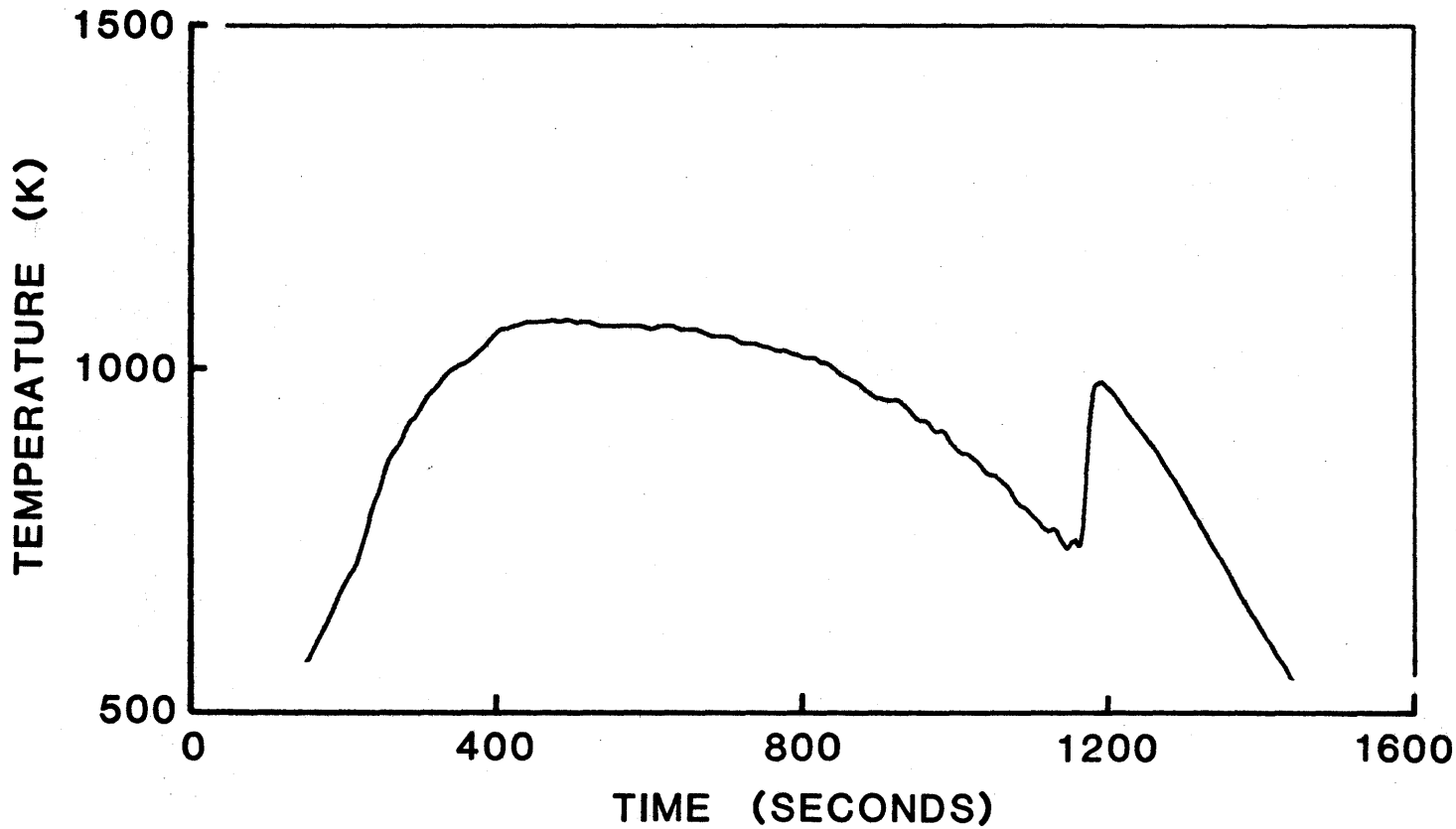

(j) x/L = 0.592

Figure 2. - Continued.

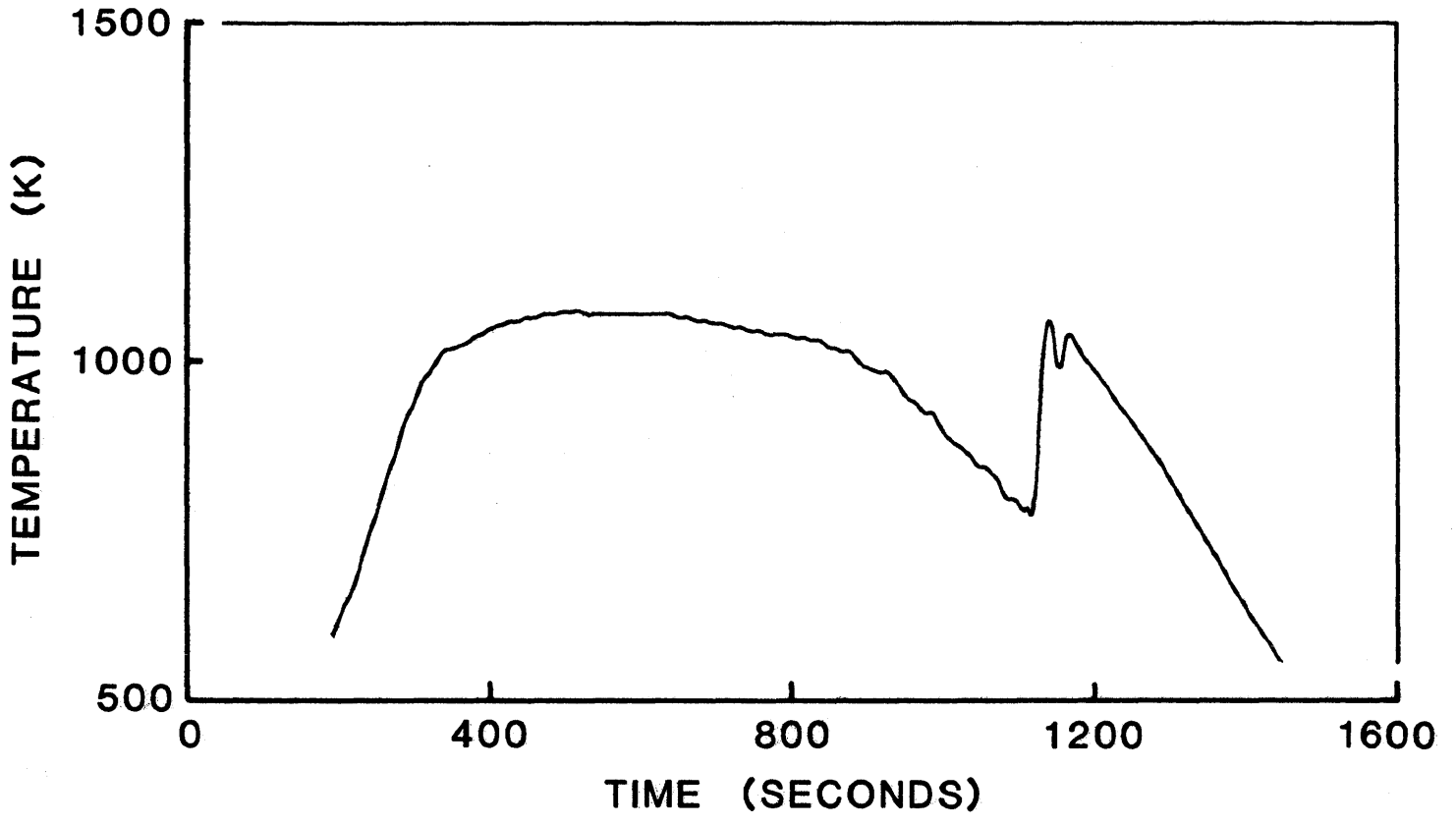

(k) x/L = 0.795

Figure 2. - Continued.

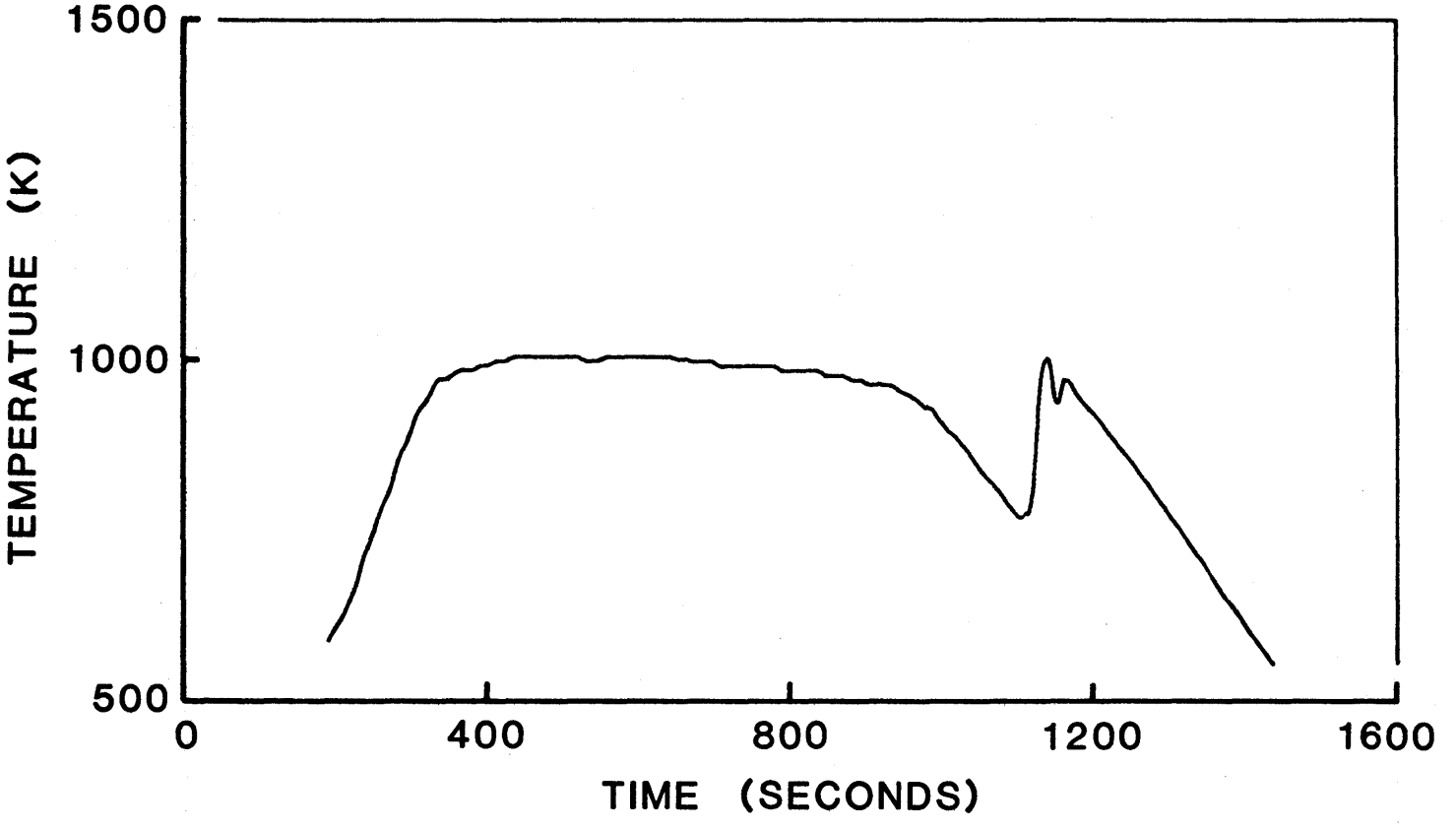

(l) x/L = 0.894

Figure 2. - Continued.

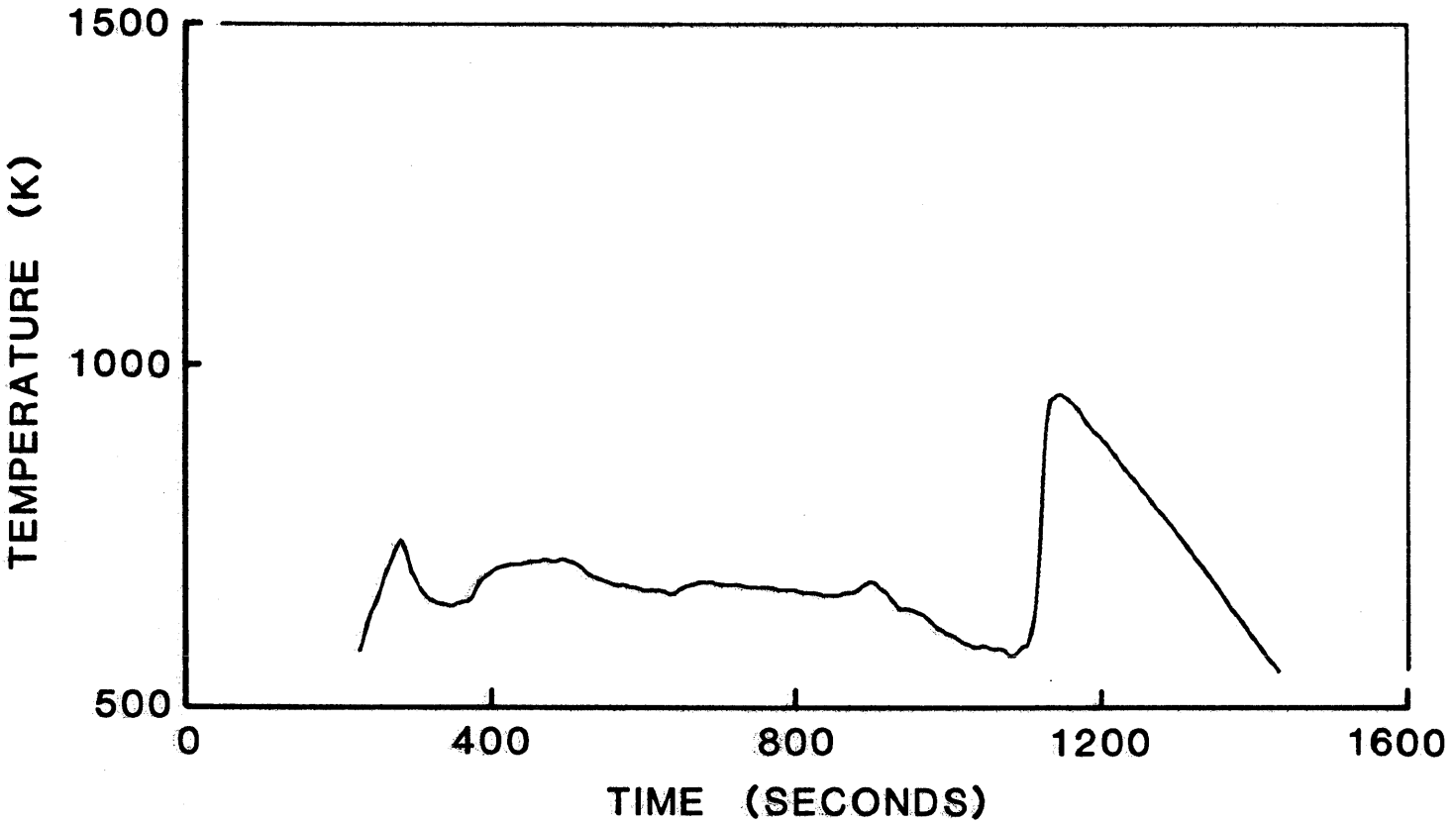

(m) x/L = 0.986

Figure 2. - Concluded.

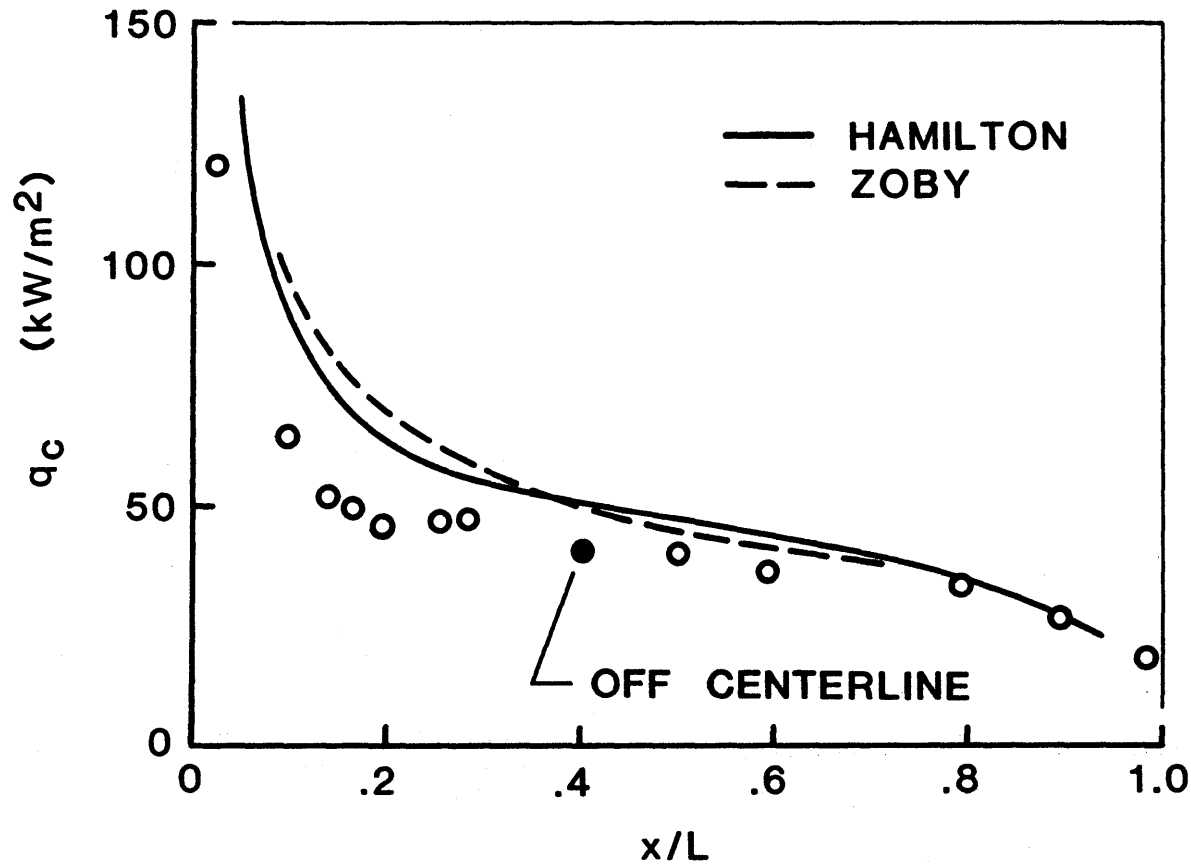

(a) Time = 270 seconds.

Figure 3. - STS-3 windward-centerline heat-transfer distributions.

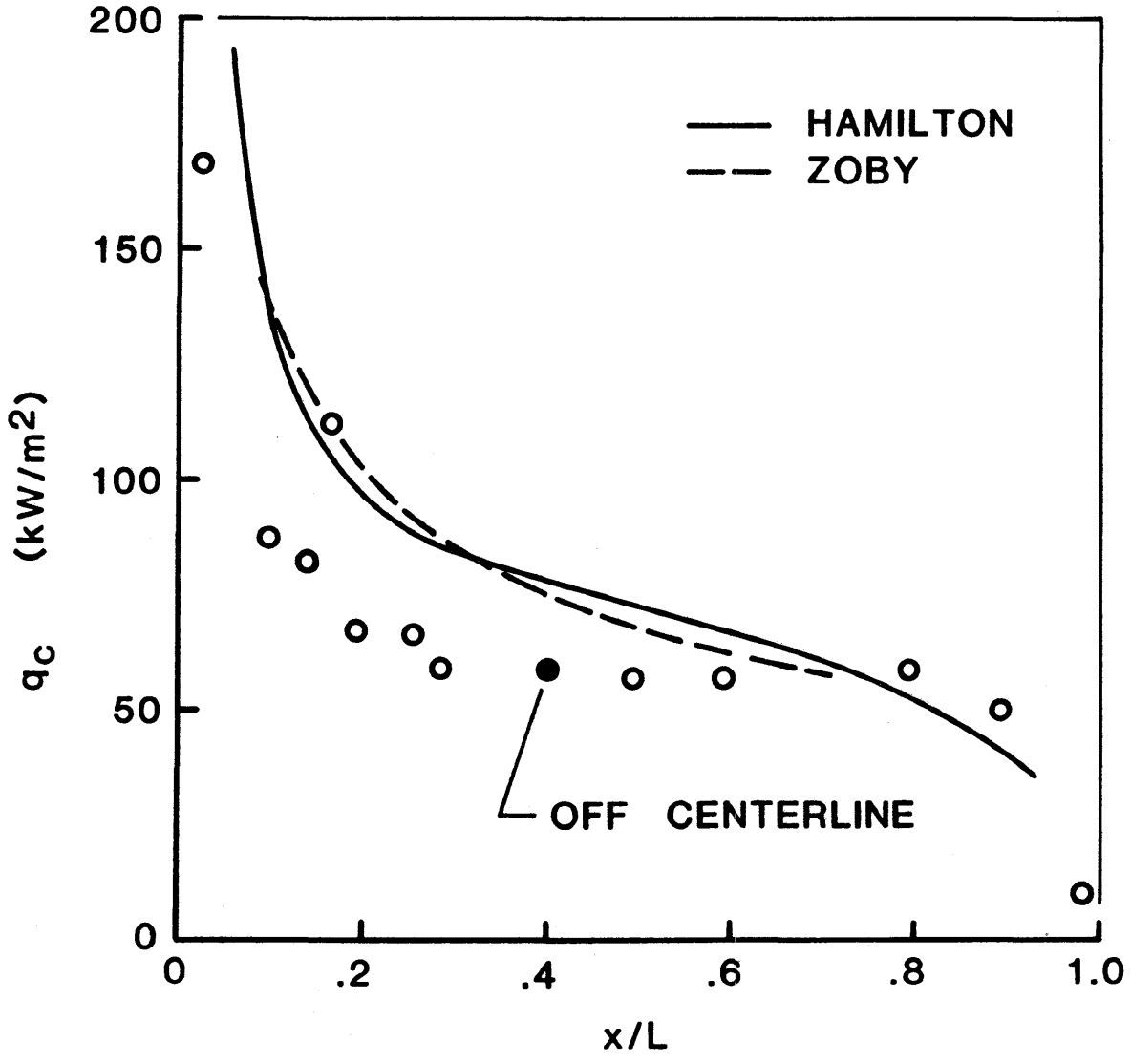

(b) Time = 350 seconds.

Figure 3. - Continued.

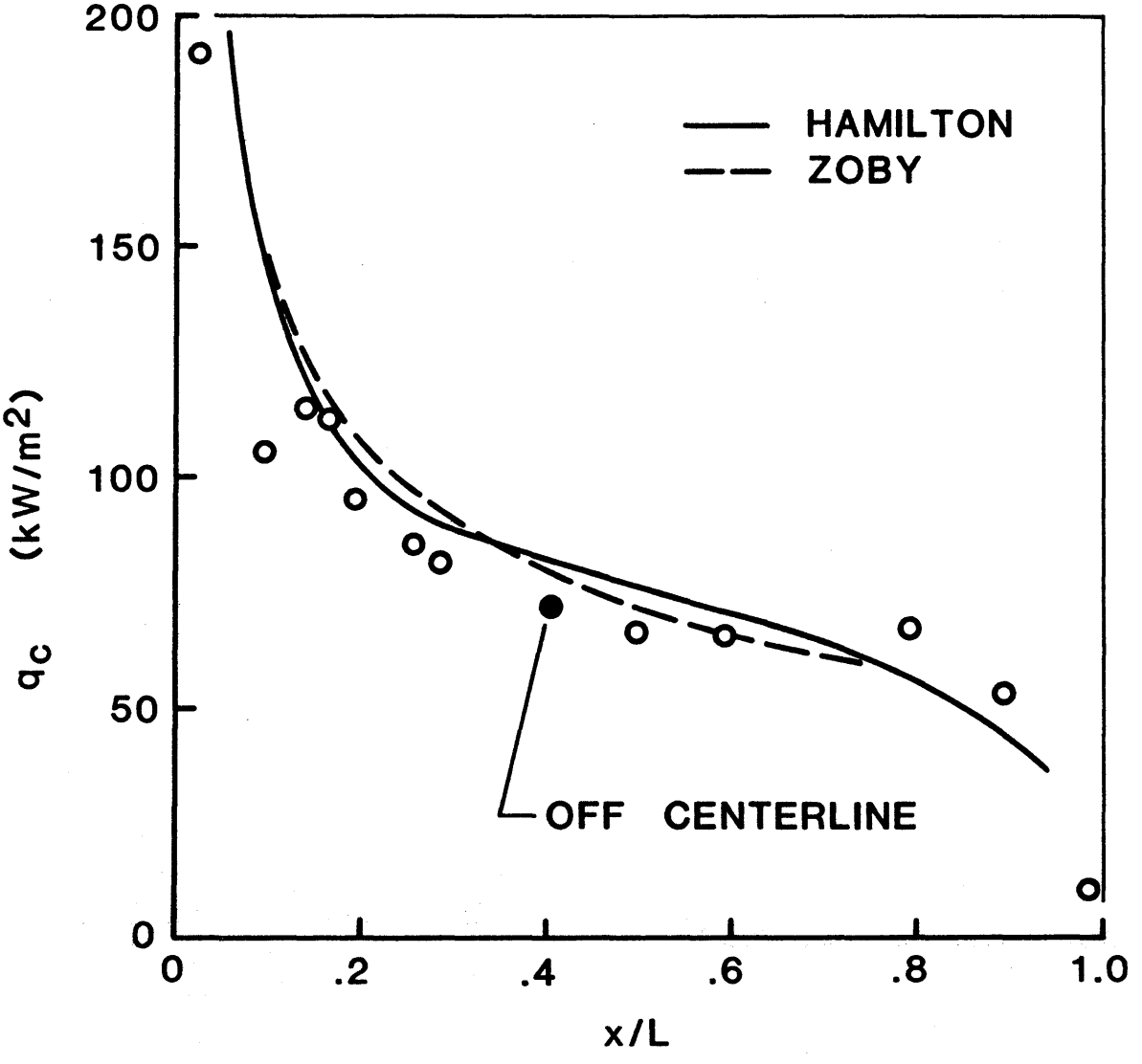

(c) Time = 640 seconds.

Figure 3. - Continued.

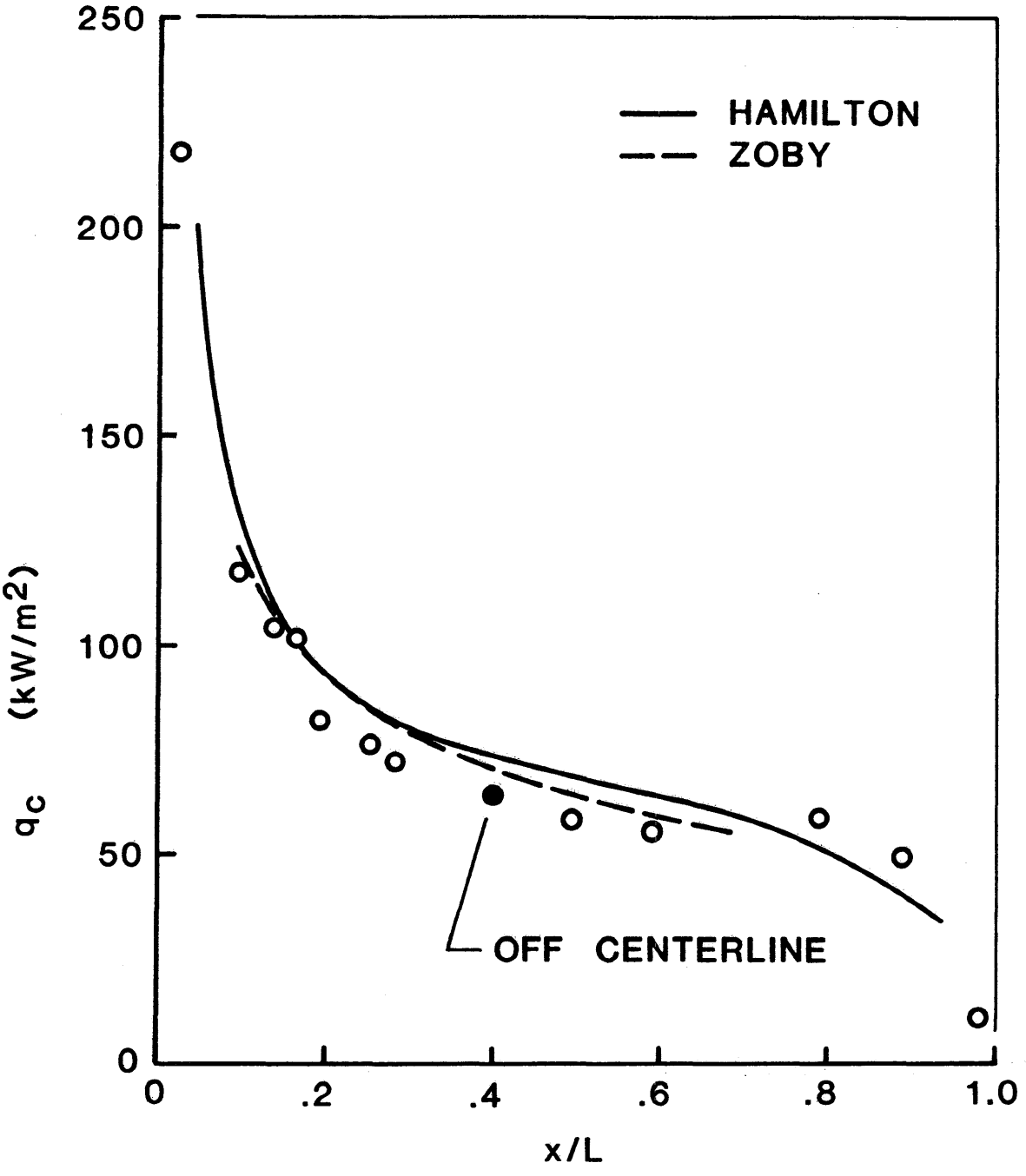

(d) Time = 825 seconds.

Figure 3. - Continued.

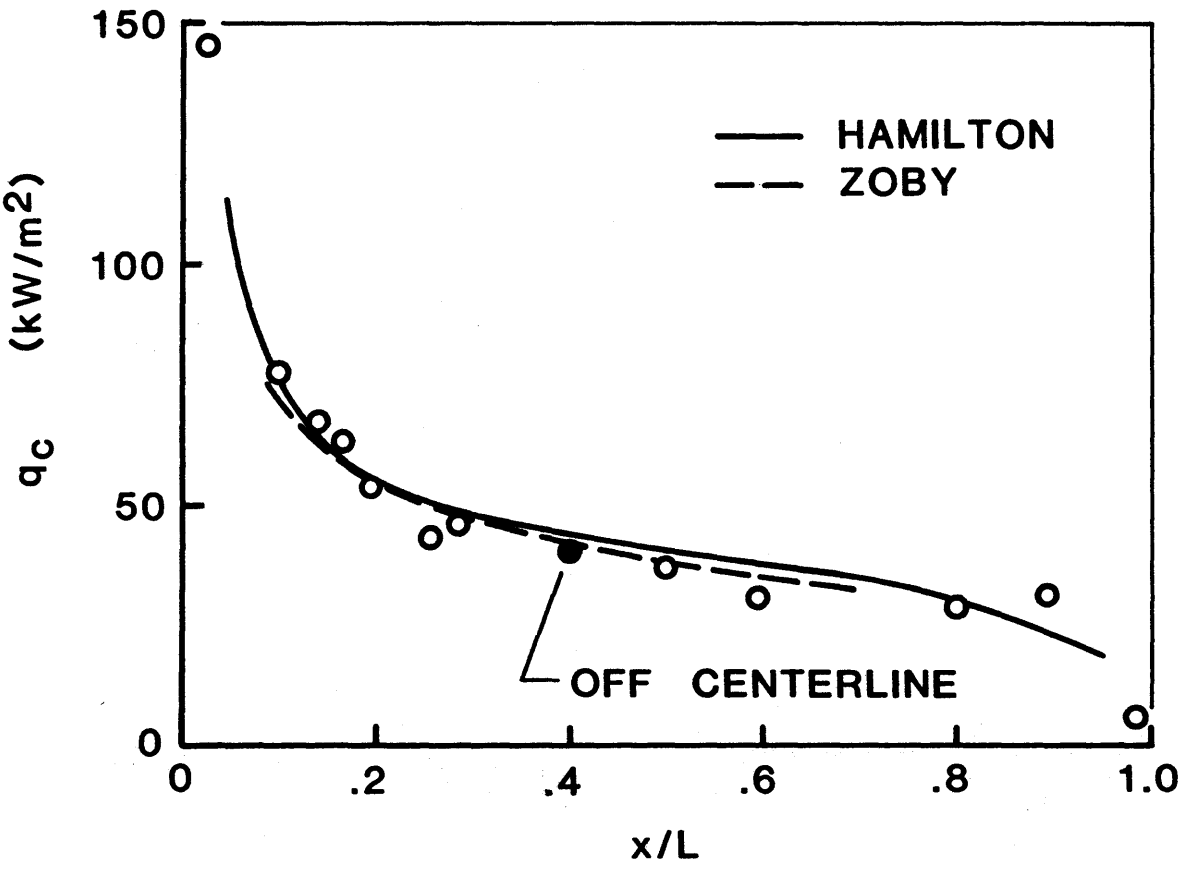

(e) Time = 1015 seconds.

Figure 3. - Concluded.

1. Report No.	2. Government Accession No.	3. Recipient's Catalog No.
NASA TM-84500		

4. Title and Subtitle	5. Report Date
Preliminary Analysis of STS-3 Entry Heat-Transfer Data for the Orbiter Windward Centerline	June 1982
	6. Performing Organization Code: 506-51-33-01
7. Author(s): David A. Throckmorton, H. Harris Hamilton II, and E. Vincent Zoby	8. Performing Organization Report No.
	10. Work Unit No.
9. Performing Organization Name and Address: NASA Langley Research Center, Hampton, VA 23365	11. Contract or Grant No.
	13. Type of Report and Period Covered: Technical Memorandum
12. Sponsoring Agency Name and Address: National Aeronautics and Space Administration, Washington, DC 20546	14. Sponsoring Agency Code

15. Supplementary Notes

16. Abstract

A preliminary analysis of heat-transfer data on the Space Shuttle Orbiter windward centerline for the STS-3 mission entry is presented. The paper includes temperature-time history plots for each measurement location, and tabulated wall-temperature and convective heating-rate data at 21 selected trajectory points. The STS-3 flight data are also compared with the predictions of two approximate methods for computing convective heat-transfer rates in equilibrium air. The paper is intended to provide the technical community with early access to a wide range of orbiter heat-transfer data.

17. Key Words (Suggested by Author(s))	18. Distribution Statement
Space Shuttle Aerodynamic heating Aerothermodynamics	Unclassified - Unlimited Subject Category 34

19. Security Classif. (of this report)	20. Security Classif. (of this page)	21. No. of Pages	22. Price
Unclassified	Unclassified	48	A03

For sale by the National Technical Information Service, Springfield, Virginia 22161